Journal Name

ROYAL SOCIETY OF CHEMISTRY

COMMUNICATION

$d^8\cdots d^{10}$ $Rh^I\cdots Au^I$ Interactions in Rh 2,6-Xylylisocyanide Complexes with $[Au(CN)_2]^-$: Bond Analysis and Crystal Effects

Verónica Conejo-Rodríguez,[a] Marconi N. Peñas-Defrutos,[a] and Pablo Espinet[a],*

The well known $[RhL_4]_n(anion)_n$ structures, with $Rh^I\cdots Rh^I$ $d^8\cdots d^8$ interactions, are replaced by others with $Rh^I\cdots Au^I$ $d^8\cdots d^{10}$ interactions such as $[\{RhL_4\}\{Au(CN)_2\}]$ (L = 2,6-Xylylisocyanide) or $[\{RhL_4\}\{Au(CN)_2\}\{RhL_4\}\{Au_2(CN)_3\}\cdot4(CHCl_3)]_\infty$ when the anion is $[Au(CN)_2]^-$. Orbital (Rh···Au), coulombic, and *inter-unit* π-π aryl stacking interactions stabilize these crystal structures.

The linear dicyanoaurate(I) anion, commercially available as $K[Au(CN)_2]$, has tendency to form $[Au(CN)_2^-]_n$ oligomers with Au···Au interactions in concentrated solutions. These oligomers are colourless but display interesting photochemical properties.[1] Au···Au interactions are also produced in Magnus-type gold salts such as $[Au(NHC)_2][Au(CN)_2]$.[2]

Similarly, although for different reasons, isocyanide rhodium(I) complexes $[Rh(CNAr)_4](A)$ (A = anion; Ar = aryl) show a marked tendency to cation association, producing dimeric $[Rh_2(CNAr)_8]^{2+}$ or trimeric $[Rh_3(CNRAr)_{12}]^{3+}$ cations with Rh···Rh interactions, both in concentrated solutions and/or in solid-state structures. There is plenty of information about these associations,[3] which give rise to dramatic colour changes, often evolving from yellow in the monomers to orange-red in the dimers and green or deep blue in the trimers. Larger associations can be induced: $[Rh(CNXylyl)_4](A)$ ($A^- = Cl^-$, ½ $SO_4^=$, F^-; Xylyl = 2,6-Xylyl) complexes self-assemble in water into ultra-long electronically active crystalline nanowires.[4]

Since the appropriate Rh^I (d^8) and Au^I (d^{10}) complexes have this tendency to establish homometallic interactions, it looked interesting to us to examine their possible combination.

Complex $[Rh(CNXylyl)_4](BF_4)$ (**1**) was synthesized from $[Rh(COD)_2](BF_4)$ and CNXylyl. Yellow crystals of **1** were obtained by slow diffusion of diethyl ether into a chloroform solution of the compound. The most prominent feature of the square-planar structure of **1** is that three of the aryl rings are almost coplanar with the coordination square plane, while the fourth aryl arranges orthogonal to this plane, forced by steric congestion (Figure 1, left).[5] The non-coplanarity in **1** facilitates a structural void to host the BF_4^- counteranion.
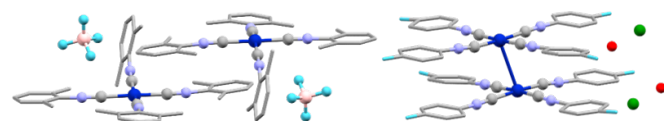

Figure 1. Left: Ball and stick structure of yellow $[Rh(CNXylyl)_4](BF_4)$ (**1**). Right: structure of $[Rh(CNC_6H_4F)_4]Cl\cdot(OH_2)$ from data in Cambridge Data Base. Blue: Rh; Green: Cl; Red: OH_2.

The reported crystal structure of the blue complex (597 nm absorption) $[Rh(CNC_6H_4F)_4]Cl\cdot(OH_2)$ (Figure 1, right),[6] shows coplanar C_6H_4F aryls favouring *intra-unit* π-π stacking. In contrast $[Rh(CNC_6H_4F)_4](ClO_4)$ is yellow and its structure contains monomeric complex units. Thus, the crystallographic structure controls the formation of Rh···Rh interaction and the appearance of colour. The energy due to π-π stacking dispersion stabilizes the close packing of the Rh cations by pairs (Rh···Rh = 3.293 Å), while the Rh···Rh interaction affords only 10-20% of the total binding energy.[7,8]

A product with $[Rh(CNXylyl)_4][Au(CN)_2]$ (**2**) stoichiometry was prepared according to eqn. 1.

$$[Rh(CNXylyl)_4](BF_4) + K[Au(CN)_2] \xrightarrow[\text{3 h, rt}]{\text{acetone/H}_2\text{O}} [Rh(CNXylyl)_4][Au(CN)_2] + K(BF_4) \quad (1)$$
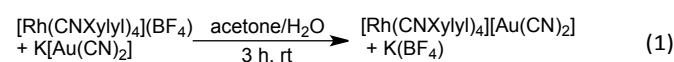
Crystallisation of **2** yielded three kinds of differently coloured crystals and structures (Figure 2), depending on the crystallisation conditions: orange crystals (**2a**), very predominant from $CHCl_3$ solutions; blue crystals (**2b**), from acetone solutions; and green crystals (**2c**) mixed with blue crystals (**2b**), from CH_2Cl_2 solutions. Their competitive formation suggests similar overall stability for the three.

[a]. IU CINQUIMA/Química Inorgánica, Facultad de Ciencias, Universidad de Valladolid, 47071-Valladolid, Spain. E-mail: espinet@qi.uva.es
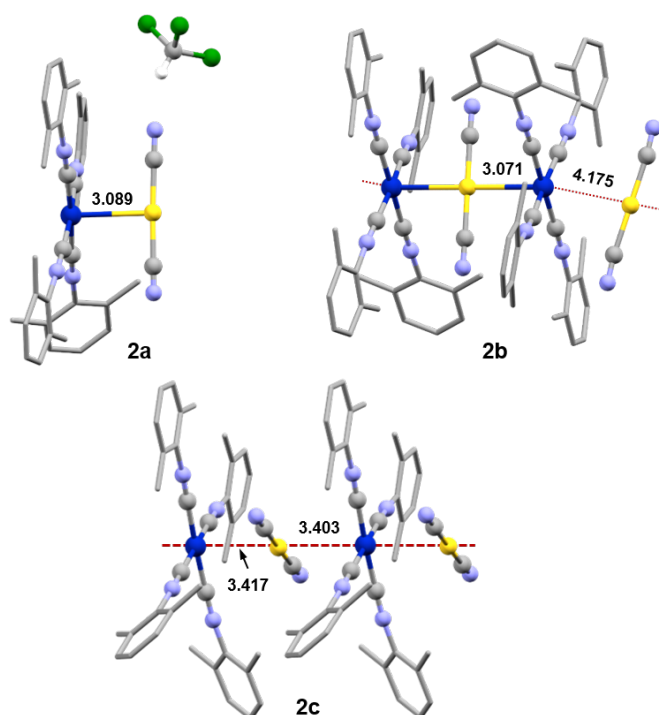
Figure 2. X-ray structures of orange **2a**, blue **2b**, and green **2c**. One CHCl$_3$ molecule per Au(CN)$_2^-$ group is found in **2a**. Observed Rh···Au distances in Å.

Structure **2a** consists of binuclear Rh···Au units, with d(Rh···Au) = 3.089 Å. Structure **2b** shows an infinite arrangement of [RhL$_4$···Au···RhL$_4$]$^+$ trinuclear units with (d(Rh···Au) = 3.071 Å), reasonably aligned with [NC–Au–CN]$^-$ anions at d(Rh···Au) = 4.175 Å. Finally, **2c** features an infinite 1D [···RhL$_4$···Au···] sequence with very similar d(Rh···Au) distances: 3.403 and 3.417 Å. In **2c**, two Xylyl aryls are out of the coordination plane. The change from polymorph **2b** to **2c** could be considered a structural symmetrisation under compensated crystalline forces in the two crystal packing patterns.

The fourth compound displaying Rh^I···Au^I interactions is [{L$_4$Rh}{Au(CN)$_2$}][{RhL$_4$}{Au$_2$(CN)$_3$}·4(CHCl$_3$)]$_\infty$ (**3**), which was crystallized as a very minor product from the CHCl$_3$ solutions prepared to obtain single crystals of **2a** (Figure 3).
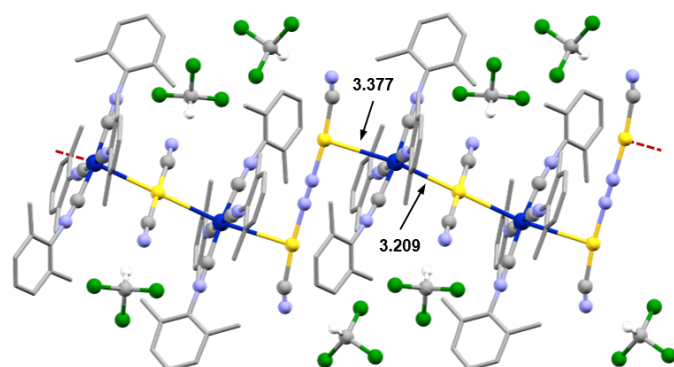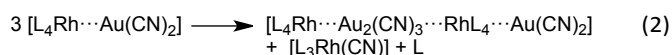

Figure 3. Ball and stick structure of the violet compound [{L$_4$Rh}{Au(CN)$_2$}][{RhL$_4$}{Au$_2$(CN)$_3$}·4(CHCl$_3$)]$_\infty$ (**3**). Observed Rh···Au distances in Å. C or N in the bridging CN group of [Au$_2$(CN)$_3$]$^-$ cannot be assigned. Two CHCl$_3$ molecules per [Au(CN)$_2$]$^-$ or [Au$_2$(CN)$_3$]$^-$ group are observed.

A most striking feature of **3** is the appearance of the [Au$_2$(CN)$_3$]$^-$ anion bridging [RhL$_4$···Au···RhL$_4$]$^+$ units and making an infinite (···RhL$_4$···Au(CN$_2$)···RhL$_4$···Au(CN)–(C/N)–Au(CN)···)$_\infty$ zigzag chain. Compounds with anions [Au(CN)$_2$]$^-$ are common, and there is also one report of encapsulated [Au$_3$(CN)$_4$]$^-$,[9] but [Au$_2$(CN)$_3$]$^-$ has never been reported before.[10]

The crystal of **3** contains CHCl$_3$ molecules, which are connected by N···H hydrogen bonds to the cyano groups of [Au(CN)$_2$]$^-$ and to the terminal ones of [Au$_2$(CN)$_3$]$^-$. The X-ray study cannot individualize the C or the N atom in the bridging cyano group of [Au$_2$(CN)$_3$]$^-$ because they are submitted to non resoluble disorder (this is represented as Au–(C/N)–Au. The two different Rh···Au distances observed in **3**, whether to [Au(CN)$_2$]$^-$ (3.209 Å) or to [Au$_2$(CN)$_3$]$^-$ (3.377 Å), are somewhat shorter that in the other polymeric species **2c**, but longer than in **2a** and **2b**.

[Au$_2$(CN)$_3$]$^-$ is not formed by adventitious traces of acid in the solvent removing the missing CN$^-$ as HCN, since the crystals of **2a** are resistant to fairly concentrated hydrochloric acid. A very plausible alternative is that the missing CN$^-$ is captured by [RhL$_4$]$^+$ (Equation 2). As a matter of fact, reaction of [RhL$_4$]Cl with NaCN gives quantitatively [Rh(CN)L$_3$] (**4**) + L + NaCl (see ESI). Considering the scarcity of crystals of **3** formed, the small accompanying mass of [Rh(CN)L$_3$], expected to be formed according to Equation 3, would hardly be detected.

$$3\,[L_4Rh \cdots Au(CN)_2] \longrightarrow \begin{array}{l} [L_4Rh \cdots Au_2(CN)_3 \cdots RhL_4 \cdots Au(CN)_2] \\ + \ [L_3Rh(CN)] + L \end{array} \quad (2)$$

The relevant common feature of the four structures is that the Rh···Rh interactions are absent in favour of Rh···Au orbital and ionic interactions. Probably the steric difficulty of the Xylyl groups to become coplanar contributes to disfavour the formation of Rh2 species and opens the opportunity to RhAu species. The structures observed differ in the roles played by the [Au(CN)$_2$]$^-$ or [Au$_2$(CN)$_3$]$^-$ moieties, which are not that of a simple anion such as BF$_4^-$ does in **1**: they participates in formation of Rh···Au interactions at different lengths in the range 3.0–3.5 Å. Average, the linear [Au(CN)$_2$]$^-$ or [Au$_2$(CN)$_3$]$^-$ groups are located with the Au centre on the Rh atom (or close to it for the anionic [Au(CN)$_2$]$^-$ in **2b**), and in a plane approximately bisecting the *cis*-(L–Rh–L) angles. The crystal colours, and the Rh-Au distances for **1**, **2a-c**, and **3** are gathered in Table 1.

Table 1. Rh···Au interaction lengths [Å]

Compound (crystal colour) L = CN-2-6-Xylyl	Rh···Au [Å]
[L$_4$Rh](BF$_4$) (**1**) (Yellow)	–
[{L$_4$Rh}{Au(CN)$_2$}]·CHCl$_3$ (**2a**) (Orange)	3.089
[{L$_4$Rh}{Au(CN)$_2$}{RhL$_4$}](Au(CN)$_2$) (**2b**) (Blue)	3.071, 4.175
[{L$_4$Rh}{Au(CN)$_2$}]$_\infty$ (**2c**) (Green)	3.403, 3.417
[{L$_4$Rh}{Au(CN)$_2$}{RhL$_4$}{Au$_2$(CN)$_3$}·4(CHCl$_3$)]$_\infty$ (**3**) (Violet)	3.209, 3.377

All the Rh···Au distances observed are below the sum of van der Waals radii (4.89 Å), but also well above the sum of covalent radii Rh^I+Au^I (2.75 Å). They range from short

　　　　　　　　　　　　　　　　　　　　　　　　　　　　　　　　　　COMMUNICATION

distances close to 3.1 Å, where significant orbital overlapping and some orbital Rh[I]···Au[I] contribution to the stability of the crystal can be presumed, to long distances of 4.175 Å, where the Rh[I]···Au[I] bond orbital contribution to crystal stabilization must be negligible.

At variance with [Rh$_2$(CNAr)$_8$]$^{2+}$ dimers,[7] in this collection of RhAu complexes the Au moiety does not bear aryl substituents, hence *intra-unit* π-π stacking interactions to support the Rh[I]···Au[I] interactions cannot be formed. However, we should keep in mind that we are discussing structures only existing in the tridimensional crystal, where multiple *inter-units* π-π stacking interactions observed in the X-ray structures (involving aryls of neighbouring Rh···Au units in the crystal and not susceptible to simple description and analysis; see Figure ESI9) on one hand, and the sum of Coulombic interactions on the other are probably the higher contributors to the structure adopted in the crystal.[11,12] Although the Rh[I]···Au[I] short distances are powerfully catching the eye in Figures 2 and 3, the small Rh[I]···Au[I] orbital contribution is not *determining* of the structure, but *determined* by the structure.

Regardless of their strength, DFT MO examination of the d^8···d^{10} Rh···Au orbital interactions is interesting, and is needed to understand the colours observed. This study can be qualitatively approached at low computational cost on a simplified model in gas-phase. The condition is that the Rh···Au distance is an experimental fact that must be respected.[13] This condition was applied first to **2a**, applying single-point calculations to the X-ray structure, with a fixed 3.089 Å Rh···Au distance (details in ESI). The resulting orbitals more heavily involved in the intermetallic interactions are shown in Figure 4.
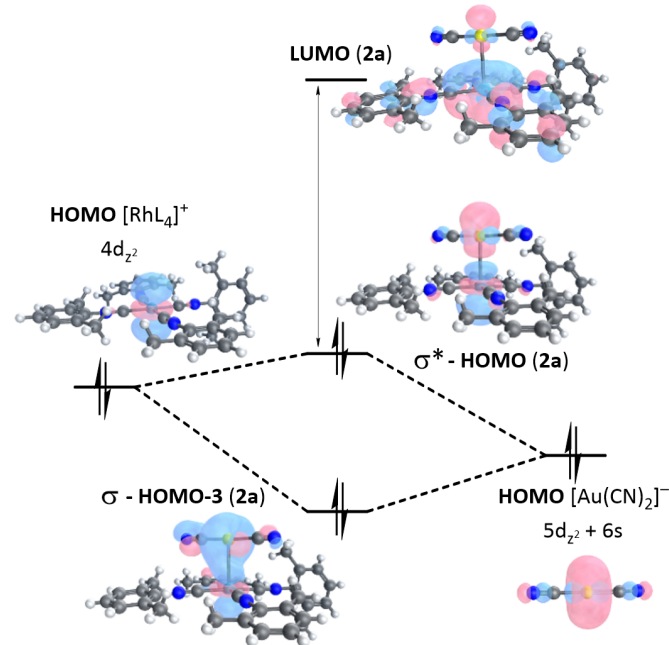

Figure 4. σ-HOMO-3 and σ*-HOMO orbitals for the intermetallic interaction, from the HOMO orbitals of the two interacting ions. The energies are arbitrary but we assume that the HOMO of [Au(CN)$_2$]$^−$ is somewhat more stable than that of [RhL$_4$]$^+$ since: a) in the starting reagents the Mulliken positive charge on Au (0.516 e$^−$) is larger than that on Rh (0.369 e$^−$); b) in complex **2a** the charges are 0.477 e$^−$ for Au and 0.403 e$^−$ on Rh, supporting neat electron transfer from Rh to Au.

The HOMO of [Rh(CNXylyl)$_4$]$^+$ is a 4d$_{z^2}$(Rh) orbital and the HOMO of [Au(CN)$_2$]$^−$ is mostly 5d$_{z^2}$ + 6s (Au) provide in **2a** the bonding σ-HOMO-3(RhAu) and the antibonding σ*-HOMO(RhAu) combinations, which resemble those of Rh[I]···Rh[I] or Au[I]···Au[I] systems.[1,3,14] Overall, they give rise to some net Rh[I]···Au[I] bonding interaction, even if this stabilizing effect is modest. Since the participation of Au in the bonding HOMO-3 is larger than that of Rh (see computational details in ESI), this interaction produces some neat electron transfer from Rh to Au, as suggested by the Mulliken charges (in caption to Fig. 4).

The UV-vis spectra of the solids were recorded on drop-cast films and follow the typical trends of Rh[I] oligomers with Rh[I]···Rh[I] interactions.[3] Representative spectra are plotted in Figure 5. Possibly these films contain more than one structure but they are sufficient to examine the effect of Rh[I]···Au[I] interactions. In similarity with the Rh[I]···Rh[I] systems, bands at higher wavenumbers are seen when structures with Rh[I]···Au[I] short distances are present, and the effect increases the higher the involvement of these interactions.
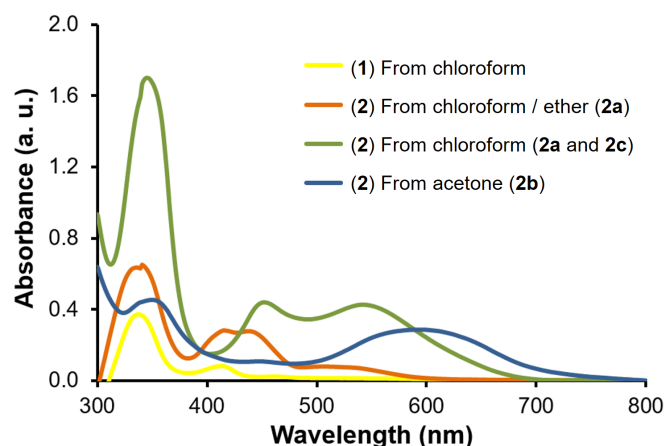

Figure 5. UV-vis absorptions in drop-cast films from solutions of **1** and **2a-c**.

Complexes **1** and **2a-c** show intense bands below 400 nm associated to intraligand absorptions and intermediate bands associated to 4dz^2(Rh) → 5p transitions.

In the Rh dimers, the lower energy bands above 450 nm originate from the 4dσ*(Rh2) HOMO orbital (the antibonding combination of the 4dz^2 orbitals) transferring charge to the LUMO 5pσ(Rh2)/π*(isocyanide) orbital.[3] In our RhAu complexes the LUMO(RhAu) orbital for **2a** is the combination of the equivalent 5p(Rh)/π*(isocyanide) with 6p(Au), which is Rh-Au antibonding (Figure 4). Thus, although the Au centre only scarcely contributes to it, the Rh centre involves the π orbitals of its isocyanide ligands in the lowest energy transition, which gives rise to an orange colour for **2a**.

The σ* HOMO **2b** (RhAuRh) in Figure 6 (left) shows a multiply antibonding combination destabilizing the orbital, lowering of the HOMO-LUMO (RhAuRh) energy gap, and consequently displacing the charge transfer band to higher wavenumbers compared to **2a**. In effect, blue colour is observed in the crystals of **2b**, and its drop-cast film from acetone. The corresponding stabilization of the σ-bonding (RhAuRh) orbital (Figure ESI17) contributes to produce a short Rh···Au distance in **2b**.

The calculated gap values for **2a** (6.91 eV) and **2b** (6.15 eV) follow the expected trend but are clearly overestimated. They should be only about 2.6 and 1.9 eV, respectively, to justify the colours observed. However, the gap difference between **2a** and **2b** is quite similar, whether from DFT calculation (0.76 eV) or from colours (about 0.7 eV) suggesting that this difference is meaningful. This indicates that forces further stabilizing the LUMOs energy, relatively similar for **2a** and **2b**, are missing in the calculation. Obviously these forces must be the inter-unit π-π aryl stacking interactions in the crystal, which should stabilize the respective LUMOs by 4.3 eV for **2a** and 4.2 eV **2b** in order to bring the σ*-HOMO → LUMO transition in the crystal into the wavelength range of orange and, respectively, blue colours. Although in an indirect way, the result that the effect on the LUMOs of these inter-unit π-π stacking contributions is energetically quite similar keeps well with the fact that these structures coexist, as mentioned above.
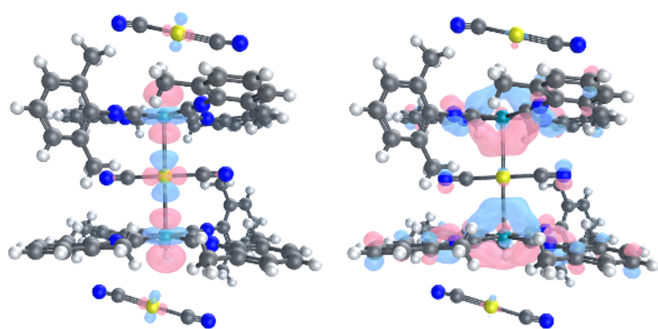

Figure 6. σ* HOMO **2b** (RhAuRh) (left) and LUMO **2b** (right) orbitals calculated for an anionic (Au··RhAuRh··Au)⁻ fragment of **2b** (for other selected orbitals see ESI).

In conclusion, the combination of d^8 [Rh(CNXylyl)$_4$]$^+$ with d^{10} [Au(CN)$_2$]$^-$ gives rise to formation of different crystals where (RhAu), (RhAuRh), or (RhAu)$_\infty$ d^8···d^{10} interactions totally prevail on alternative d^8···d^8 (RhRh) + d^{10}···d^{10} (AuAu) interactions. These compounds are not supported by intra-unit π-π aryl stacking, which suggests that the ionic contribution is taking this role to induce cation/anion Rh^I···Au^I approximation in the crystal. The orbital M-M' interactions are quite comparable, so that the effect of Au as modifier of MLCT transitions in Rh···Au complexes is qualitatively similar to the effect of a second Rh in Rh···Rh complexes. The crystals stabilization must have a large ionic contribution, but much stabilization in the crystal comes also from inter-unit π-π aryl stacking of the isocyanide aryls. This inter-unit π-π aryl stacking in the crystal is also responsible notable stabilization of the LUMO orbitals, which reduces the σ*-HOMO → LUMO energy, bringing these electron transfers into the range orange-to-blue colours.

Conflicts of interest

There are no conflicts to declare.

Notes and references

1 a) G. Cui, X.-Y. Cao, W.-H. Fang, M. Dolg and W. Thiel, *Angew. Chem. Int. Ed*., 2013, **52**, 10281–10285; b) M. Iwamura, K. Nozaki, S. Takeuchi and T. Tahara, *J. Am. Chem. Soc*., 2013, **135**, 538–541. c) S. R. Hettiarachchi, M. A. Rawashdeh-Omary, S. M. Kanan, M. A. Omary, H. H. Patterson and C. P. Tripp, *J. Phys. Chem. B*, 2002, **106**, 10058–10064; d) M. A. Rawashdeh-Omary, M. A. Omary, H. H. Patterson and J. P. Fackler, *J. Am. Chem. Soc.*, 2001, **123**, 11237–11247. e) M. A. Rawashdeh-Omary, M. A. Omary and H. H. Patterson, *J. Am. Chem. Soc.*, 2000, **122**, 10371–10380.

2 a) Q. Liu, M. Xie, X. Chang, Q. Gao, Y. Chen and W. Lu, *Chem. Commun.*, 2018, **54**, 12844–12847; b) Q. Liu, M. Xie, X. Chang, S. Cao, C. Zou, W.-F. Fu, C.-M. Che, Y. Chen and W. Lu, *Angew. Chem. Int. Ed.*, 2018, **57**, 6279 –6283.

3 a) V. W.-W. Yam, V. K.-M. Au and S. Y.-L. Leung, *Chem. Rev.*, 2015, **115**, 7589–7728 and references therein; b) A. K.-W. Chan, K. M.-C. Wong and V. W.-W. Yam, *J. Am. Chem. Soc.*, 2015, **137**, 6920–6931.

4 Y. Chen, K. Li, H. O. Lloyd, W. Lu, S. S.-Y. Chui and C.-M. Che, *Angew. Chem. Int. Ed.*, 2010, **49**, 9968 –9971.

5 An alternative structure of the cation, with the four Xylyl rings making dihedral angles with the coordination plane in the range 19.3-45.6°, was found in the yellow (BPh$_4$)$^-$ salt: T. V. Ashworth, D. C. Liles, H. E. Oosthuizen and E. Singleton, *Acta Cryst.*, 1984, **C40**, 1169 – 1172.

6 H. Endres, N. Gottstein, H. J. Keller, R. Martin, W. Rodemer and W. Steiger, *Z. Naturforsch.*, **34b**, 827–833.

7 S. Grimme and J.-P. Djukic, *Inorg. Chem.*, 2011, **50**, 2619–2628.

8 As an example, DFT calculations for [Rh$_2$(CNPh)$_8$](PF$_6$)$_2$ in the gas-phase (reference 7) show that the contribution of Rh···Rh interactions to stabilization of the dimer is small (about 10-15% relative to the total binding energy).

9 W. Meng, A. B. League, T. K. Ronson, J. K. Clegg, W. C. Isley III, D. Semrouni, L. Gagliardi, C. J. Cramer and J. R. Nitschke, *J. Am. Chem. Soc.*, 2014, **136**, 3972–3980.

10 In contrast, there are many examples of presence of [Ag$_2$(CN)$_3$]$^-$ in structures with [Ag(CN)$_2$]$^-$, always observed minority crystalline products. The formation of [Ag$_2$(CN)$_3$]$^-$ has not been convincingly explained and its existence seems to require its involvement in some crystalline structure. See for example: a) H.-B. Zhou, W. Dong, M. Liang, D.-Z. Liao, Z.-H. Jiang, S.-P. Yan and P. Cheng, *Z. Anorg. Allg. Chem.*, 2004, **630**, 498–500. b) J. R. Stork, D. Rios, D. Pham, V. Bicocca, M. M. Olmstead and A. L. Balch, *Inorg. Chem.*, 2005, **44**, 3466–3472.

11 X.-G. Xiong, Y.-L. Wang, C.-Q. Xu, Y.-H. Qiu, L.-S. Wang and J. Li, *Dalton Trans.*, 2015, **44**, 5535–5546.

12 S.-G. Wang and W. H. E. Schwarz, *J. Am. Chem. Soc.*, 2004, **126**, 1266–1276.

13 The dispersion corrected hybrid functional ωB97X-D was used. If free geometry relaxation in gas phase is allowed, the two metal centres separate (see ESI). Thus, the restriction imposed is needed to account for the structure existing in the crystals.

14 M. M. Conradie, P. H. van Rooyen, C. Pretorius, A. Roodt and J. Conradie, *J. Mol. Struct.* 2017, **1144**, 280–289.